Control of the multiferroic transition in $Ni_3V_2O_8$ by transition metal doping

A. Kumarasiri and G. Lawes[*]

Department of Physics and Astronomy, Wayne State University, Detroit, Michigan 48201, USA
(Received 7 June 2011; revised manuscript received 1 August 2011; published 31 August 2011)

We have studied the effects of doping magnetic ions on the phase transitions in polycrystalline $Ni_3V_2O_8$ samples using magnetic, dielectric, and specific heat measurements. Substituting spin-1/2 Cu results in a larger suppression of the transition temperatures than observed on doping with spin-3/2 Co. The multiferroic-ordering transition persists at small concentrations for both Co and Cu dopants, with this phase still developing at concentrations of almost 30 at% Co. However, the multiferroic-magnetic structure is completely suppressed at only 10 at% Cu. On the Co-rich side of the composition, we find that the magnetic-ordering temperatures for $Co_3V_2O_8$ are suppressed rapidly with Ni doping. We present phase diagrams for $(Ni_{1-x}M_x)_3V_2O_8$ (M = Cu and Co). These studies suggest that the spin structures in $Ni_3V_2O_8$ responsible for the development of ferroelectric order are relatively robust against perturbations produced by magnetic dopants, with the most significant disruption of the magnetic structure developing for Cu doping.

There is considerable interest in understanding the materials' properties underlying the development of simultaneous magnetic and ferroelectric order in multiferroics. As a first step in creating a taxonomy for these materials, a large number of magnetoelectric multiferroics have been identified and investigated in recent years.[1,2] One of the most widely studied classes are the rare earth (R) manganites, including perovskite $RMnO_3$[3–6] and RMn_2O_5.[7,8] $BiFeO_3$, a room temperature multiferroic having ferroelectric and magnetic transitions at ~1100 K and ~640 K, respectively, has also been investigated in great detail.[9–11] One technique for exploring the mechanisms producing multiferroic order is to selectively dope a material and characterize the associated changes in the structural, magnetic, or ferroelectric properties. The manner in which the dopants perturb the materials' properties will, in general, depend on the specific mechanisms producing the multiferroic order. As an example, the multiferroic $RMnO_3$ systems have an orthorhombically distorted perovskite structure where the ferroelectric order is driven by the magnetic interactions. Substitution at the R site can induce distortions in the lattice, changing the M-O-M bond angle and hence the magnetic-exchange interaction, which finally changes the magnetic and ferroelectric properties.[6]

Selective doping using magnetic and nonmagnetic ions is expected to provide important insight into the development of magnetic and ferroelectric order. In the following we focus on $Ni_3V_2O_8$, a frustrated Kagome staircase material in which the ferroelectric transition and a magnetic transition occur simultaneously.[12] The $Ni_3V_2O_8$ lattice contains two inequivalent Ni^{2+} sites, as can be seen in Fig. 1(a). These inequivalent sites are referred to as spine and cross-tie sites. $Ni_3V_2O_8$ orders magnetically at $T_H = 9.1$ K into the high temperature incommensurate (HTI) spin structure where the Ni^{2+} spins on the spine sites arrange predominantly along the crystallographic a axis. At $T_L = 6.3$ K, there is an inversion symmetry-breaking magnetic-phase transition into the low temperature incommensurate (LTI) structure, which is simultaneously antiferromagnetic and ferroelectric. Here both spine and cross-tie spins rotate within the a-b plane. This inversion symmetry breaking vanishes at 3.9 K when the system enters a canted antiferromagnetic (CAF) phase, followed by another transition at 2.1 K into a slightly different CAF phase.[12,13]

$Ni_3V_2O_8$ provides a good platform for investigating doping effects in multiferroics having strongly coupled magnetic and ferroelectric properties, since the spin structures and phase diagram for this material are well understood[12,13] and there is only one magnetic ion present, the spin-1 Ni^{2+} ions. However, there is still no definitive understanding of the origin of the spin-charge coupling in $Ni_3V_2O_8$. Some of the models proposed include a phenomenological model suggesting the spin-phonon coupling is responsible[14] and provide some specific phonon modes that could be involved. Other studies have also found evidence for significant spin-lattice coupling in this system.[15] We have previously investigated the effects of nonmagnetic Zn doping, which indicated that the multiferroic transition persisted even with 30 at% Zn doping, although the magnetic transition temperatures were suppressed linearly with doping fraction consistent with expectations from percolation models.[16] Similar studies have been done on $MnWO_4$, where magnetic Mn^{2+} ions were substituted by nonmagnetic Zn and Mg. In these investigations it was observed that the phase transition temperatures were also suppressed linearly with doping fraction.[17] Another recent study finds that the multiferroic phase of $MnWO_4$ is also remarkably stable against such doping by nonmagnetic ion, which persists up to a 50 at% Zn fraction.[18]

There is also considerable interest in exploring the stability of the magnetic phase diagram against magnetic dopants, since this may offer a route to improve the magnetic properties of the multiferroics. Previous studies on $(Co_xNi_{1-x})_3V_2O_8$ ceramics using magnetization and neutron diffraction measurements found evidence that the $Co_3V_2O_8$ magnetic structure is maintained only for $x > 0.98$, while the HTI $Ni_3V_2O_8$ magnetic structure is realized for $x < 0.71$.[19] Furthermore studies indicate a minimum Neel temperature of $T_N = 5.5$ K at $x \sim 0.76$.[20] Measurements on single crystal samples also suggest a cross-over between $Ni_3V_2O_8$ and $Co_3V_2O_8$ antiferromagnetic structures near $x \sim 0.8$.[21,22] A recent report on Zn-, Co-, and Mn-doped $Ni_3V_2O_8$ finds that the ferroelectric order
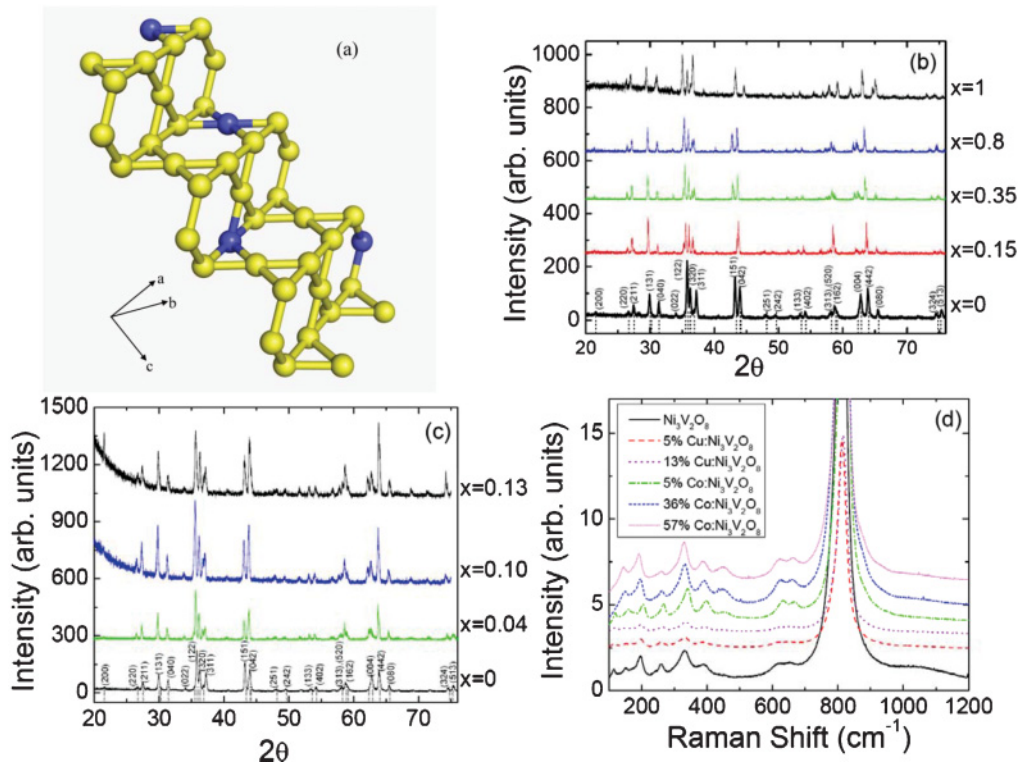
FIG. 1. (Color online) (a) Representation of a single plane of the Ni^{2+} Kagome lattice with random 10% transition metal doping, (b) XRD spectra for selected Co-substituted $Ni_3V_2O_8$ samples, (c) XRD spectra for selected Cu-substituted $Ni_3V_2O_8$ samples, and (d) Raman spectra for pure $Ni_3V_2O_8$, and Co and Cu-substituted $Ni_3V_2O_8$ at different compositions, as indicated.

becomes more stable when doped with a small amount of Co or Mn, and that the system undergoes a single magnetic phase transition when doped with larger Co fractions ($x = 0.36$).[19] Finally investigations on doping $Ni_3V_2O_8$ with magnetic Co^{2+} and nonmagnetic Mg^{2+} ions indicate that changes in the magnetocrystalline field induced by chemical disorder may significantly affect the magnetic properties of the system.[23] Studies on $MnWO_4$ doped with magnetic ions, specifically Fe, find a strong suppression of the multiferroic phase, which completely vanishes at an Fe fraction of $x = 0.05$.[24] This is in direct contrast to doping $MnWO_4$ with nonmagnetic Zn, where the multiferroic phase persists to doping fractions of $x = 0.50$.[18] Doping with Co, however, seems to have a smaller effect on the multiferroic phase transition than doping with Fe. A study done on $Mn_{0.85}Co_{0.15}WO_4$ single crystals finds the material is still clearly ferroelectric even at 15 at% Co doping.[25]

$Co_3V_2O_8$ has the same structure as $Ni_3V_2O_8$, with two inequivalent Co^{2+} ions on a staircase Kagome lattice, but exhibits different magnetic behavior.[23] At $T_N = 11.4$ K, the Co^{2+} spine-site spins arrange predominantly along the a axis leading to an antiferromagnetic structure similar to the HTI phase of $Ni_3V_2O_8$. At lower temperatures, $Co_3V_2O_8$ exhibits a commensurate AFM phase at 8.6 K, incommensurate phase at 6.8 K, and an AFM phase at 6.5 K before developing weak ferromagnetism in the ground state below 6.2 K.[26] The magnetic phase diagram of the structurally similar compound $Cu_3V_2O_8$ is rather simpler with a single antiferromagnetic transition having a weak ferromagnetic component observed at $T_N = 29$ K.[27]

In order to more fully explore the effects of doping magnetic ions on the magnetic and multiferroic properties of $Ni_3V_2O_8$, we substituted the spin-1 Ni with spin-3/2 Co and spin-1/2 Cu. Replacing the Ni with Co and Cu allows us to explore the effects of small perturbations of the local moments on the $Ni_3V_2O_8$ spin structure. As Co^{2+} and Cu^{2+} are stable in the 2+ ionization state and have ionic radii close to that of Ni^{2+}, we expected they would fit into the Ni site without significant lattice distortions. Since doping $Ni_3V_2O_8$ with Co has also been studied to great extent,[19–22] this will also allow us to directly compare our results with these studies.

We prepared polycrystalline $(Ni_{1-x}Co_x)_3V_2O_8$ powder samples over the entire composition range from $x = 0$ to 1 and $(Ni_{1-x}Cu_x)_3V_2O_8$ from $x = 0$ to 0.5 using a standard metal-organic synthesis technique.[16] The properties of these samples are to be compared with $Ni_3V_2O_8$ substituted with nonmagnetic Zn ions, which we have explored previously.[16] Figure 1(a) schematically illustrates a single layer of the Ni ions in the Kagome staircase plane with approximately 10 at% of the Ni^{2+} sites (yellow) replaced with dopant ions (blue). We chose to investigate the entire range of compositions from $x = 0$ to $x = 1$ for Co substitution to extend the $(Ni_{1-x}Co_x)_3V_2O_8$ phase diagram to include other magnetic transitions, specifically focusing on the multiferroic phase. We found that samples having larger Cu fractions tended to develop secondary phases, so we limited our investigation to smaller Cu concentrations.

We prepared the samples using a mixture of nickel (II) 2-ethylhexanoate and vanadium napthanate oxide, and then added an appropriate amount of cobalt (II) 2-ethylhexanoate

or copper (II) neodecanoate to obtain the desired composition. These precursors were dissolved in xylene then mixed in an ultrasonic bath for 30 minutes before heating to $450\,^\circ$C for 1 hour to burn off the organic compounds. The samples were subsequently heated in air to $1000\,^\circ$C for 2 hours. The resulting flakes were ground into a powder and cold pressed into pellets. The cobalt, copper, and nickel concentrations for these samples were verified by energy dispersive x-ray spectroscopy (EDS) on a Hitachi S-2400 scanning electron microscope equipped with an EDAX spectrometer and found to be in good agreement with the expected values (not shown).

We investigated the structure of these samples using x-ray diffraction (XRD) and Raman spectroscopy. Figure 1(b) shows the diffraction patterns obtained for representative $(Ni_{1-x}Co_x)_3V_2O_8$ samples over the entire composition range. For the $x = 0.15$ and $x = 0.35$ samples, all the diffraction peaks expected for $Ni_3V_2O_8$ are observed (PDF#74-1485), while the $x = 0.8$ sample has peaks corresponding to the $Co_3V_2O_8$ crystal structure (PDF#74-1487). The average crystallite size is 30 nm, calculated using the Debye-Scherrer expression. The average crystallite size and peak positions do not change significantly with x, although for $x > 0.5$ the XRD patterns show the presence of $Co_3V_2O_8$ peaks. XRD spectra for $(Ni_{1-x}Cu_x)_3V_2O_8$, plotted in Fig. 1(c), show similar results to those obtained for lower Co fractions, with no evidence for impurity phases. Here the increase of intensity at small angles for the $x = 0.1$ and 0.13 curves reflects the background contribution from a plastic sample holder; a metal sample holder, which contributes a negligible background, was used for the other samples.

We used Raman spectroscopy to confirm structure of the samples and as a sensitive test for the presence of impurity phases. Figure 1(d) shows Raman spectra obtained for $(Ni_{1-x}M_x)_3V_2O_8$ for $x = 0.05$ and 0.13 for M = Cu, and $x = 0.05$, 0.36, and 0.57 for M = Co, together with pure $Ni_3V_2O_8$. All the peaks for the doped samples correspond to those observed for pure $Ni_3V_2O_8$. These studies suggest that the samples consist solely of transition metal-substituted $Ni_3V_2O_8$, albeit with $Co_3V_2O_8$ developing at higher Co fractions, with no significant impurity phases present.

To parameterize how transition metal doping changes the magnetic properties of $Ni_3V_2O_8$, we measured the magnetization of the samples as a function of temperature under an external field of 100 Oe. The inverse magnetic susceptibility is plotted against temperature in Fig. 2(a) for four representative samples: pure $Ni_3V_2O_8$ and $Ni_3V_2O_8$ doped with 10 at% Co and Cu. These curves are linear over the temperature range plotted, and we calculate the effective moment per transition metal ion using the Curie-Weiss law, $\chi = C/(T - T_\theta)$, where $C = Ng^2\mu_B^2 J(J + 1)/3k_B$ is the Curie constant and T_θ the Weiss temperature. Here the spin-only value $(J = S)$ provides a better agreement to the measured values, which we attribute to the orbital quenching often observed in transition metal oxides. We find the effective moments, per transition metal ion, to be $3.5\,\mu_B$, $3.4\,\mu_B$, and $4.0\,\mu_B$ for undoped $Ni_3V_2O_8$ and $Ni_3V_2O_8$ doped with Cu and Co, respectively. This decrease in the effective moment on replacing spin-1 Ni^{2+} ions with spin-1/2 Cu^{2+} ions and increase in effective moment on substituting Co^{2+} ions is consistent with the expected change in the magnetic response of the system. The Curie-Weiss temperature
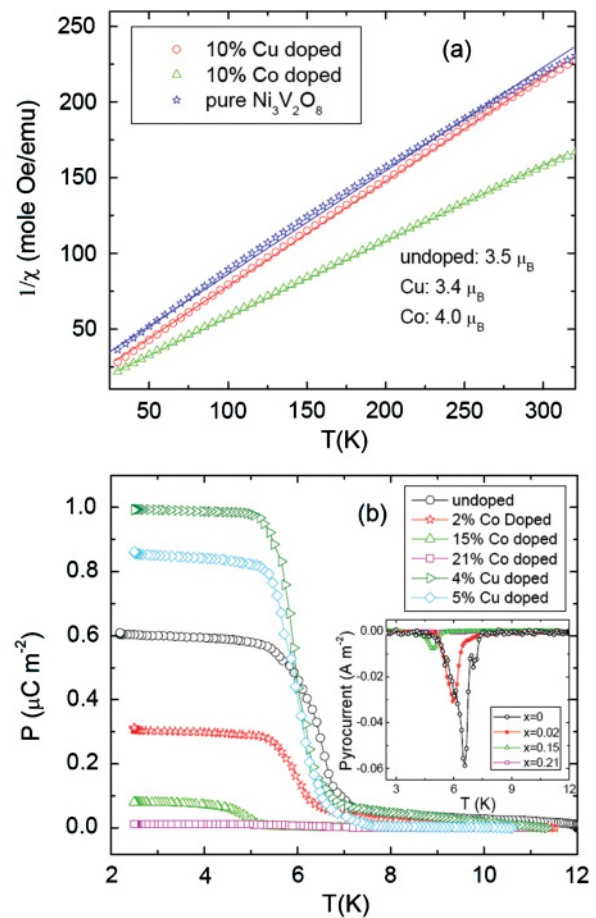

FIG. 2. (Color online) (a) Inverse magnetic susceptibility plotted as a function of temperature for pure $Ni_3V_2O_8$ and Co- and Cu-substituted $Ni_3V_2O_8$ to 10 at%. (b) Ferroelectric polarization measured for pure $Ni_3V_2O_8$ and Cu- and Co-substituted $Ni_3V_2O_8$. Inset: Pyroelectric current for pure and Co-substituted $Ni_3V_2O_8$.

for undoped $Ni_3V_2O_8$ is -32 K, which is consistent with the range of published values.[28] For the 10 at% Cu and Co-doped $Ni_3V_2O_8$, we find the Curie-Weiss temperatures are -14 K and -17.5 K, respectively. This reduction in the Curie-Weiss temperature is consistent with the lower magnetic transition temperatures in these systems.

Our primary interest is to map the full-phase diagram for transition metal substituted $Ni_3V_2O_8$ and to explore the stability of the multiferroic phase to perturbations from magnetic and nonmagnetic dopants. Of the four zero-field magnetic-phase transitions present in $Ni_3V_2O_8$, only the LTI to CAF transition at 3.9 K shows a clear magnetic signature.[13] Since we are primarily interested in understanding how the multiferroic order changes when the Ni lattice is perturbed with dopant ions, we used dielectric and heat capacity measurements to identify the different phase transitions in these samples. In order to confirm that these dielectric and thermodynamic signatures mark the onset of ferroelectric order in the doped samples, we measured the ferroelectric polarization for some of the samples. This was determined by integrating the pyrocurrent measured on warming after cooling in a poling field. Figure 2(b) plots the temperature dependence
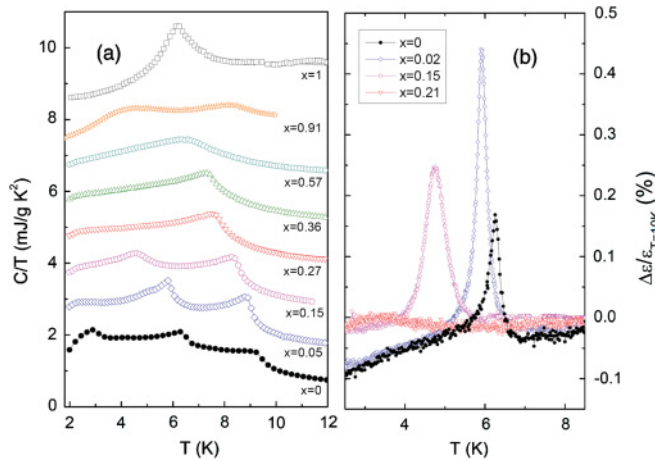
FIG. 3. (Color online) (a) Heat capacity measurements for several Co-substituted $Ni_3V_2O_8$ samples, as indicated. The curves have been vertically offset for clarity. (b) Dielectric constant measured as a function of temperature for different compositions of Co-substituted $Ni_3V_2O_8$. The values plotted are scaled to those measured at $T = 10$ K.

of the polarization of Co doped ($x = 0.02$, 0.15, and 0.21) and Cu doped ($x = 0.04$ and 0.05) $Ni_3V_2O_8$ together with that measured for undoped $Ni_3V_2O_8$ and the pyrocurrent data for some of the Co-doped samples together with pure $Ni_3V_2O_8$. We see that both samples are ferroelectric, and doping with Co and Cu has suppressed the ferroelectric transition temperature. We plot the raw pyrocurrent data for some of the Co-substituted samples, as well as for pure $Ni_3V_2O_8$, in the inset to Fig. 2(b), which allow for a more precise estimate of the transition temperature. We find a systematic reduction in the magnitude of the ferroelectric polarization on Co doping but a small increase with Cu substitution. Because the measured polarization value can depend on the electrical leakage, these polarization magnitudes may not reflect the intrinsic properties of the samples so one should avoid ascribing too much weight to the differences observed in Fig. 2(b). The ferroelectric-transition temperature found using the pyrocurrent measurements agrees well with the dielectric anomaly. However, because the sharp dielectric anomaly provides a more precise estimate of the ferroelectric-transition temperature, we used this feature to map the transition temperature rather than relying on the ferroelectric polarization.

Figure 3(a) plots the heat capacity data for a selection of the $(Ni_{1-x}Co_x)_3V_2O_8$ samples from $x = 0$ to 1 T. These were mixed with Ag powder and cold-pressed into pellets to ensure good thermal conductivity throughout the sample. The curves have been vertically shifted by 0.6 to 1 units for clarity. The heat capacity measurements for the $x = 0$ sample show the expected anomalies associated with the magnetic phase transitions in $Ni_3V_2O_8$, with the exception of the 3.9 K transition from the LTI structure to a CAF phase. There is only a very small and broad anomaly associated with this transition, which has proven to be difficult to observe in powder samples using heat capacity measurements.[16,29] With increasing Co content the transitions shift to lower temperatures, but the peak associated with the multiferroic transition remains visible until a Co fraction of $x = 0.25$. The highest temperature

anomaly, associated with the transition into the HTI phase, shows considerable broadening for $x > 0.30$ but is still visible at compositions up to $x = 0.56$. On the Co-rich side we observe two peaks in heat capacity corresponding to phase transitions at 6.1 K and 11.7 K. Although $Co_3V_2O_8$ exhibits multiple magnetic phase transitions,[30] these are the two transitions most readily discerned in heat capacity measurements on powder samples.[29] These ordering transitions are suppressed with increasing Ni fraction (decreasing values of x), with the rate of suppression being larger that observed for $Ni_3V_2O_8$ on doping with Co.

We used the dielectric anomaly associated with the development of ferroelectricity as a signature of the onset of multiferroic order. For these studies we coated the top and bottom surfaces of the pellets with silver epoxy in a parallel plate-capacitor configuration. The measurements were taken using an Agilent 4284A LCR meter at 30 kHz with temperature control provided by a Quantum Design PPMS. We plot the relative dielectric constant relative to the value at $T = 10$ K for selected samples as a function of temperature in Fig. 3(b). The undoped $Ni_3V_2O_8$ pellet exhibits a clear dielectric anomaly at $T = 6.3$ K that marks the transition from the paraelectric HTI phase to the multiferroic LTI phase. Similar anomalies are observed with increasing Co content, although the peaks become broader and shift towards lower temperatures. While this multiferroic transition temperature is suppressed, consistent with the thermodynamic measurements, the magnetic structure giving rise to ferroelectric order apparently persists to Co fractions of at least 20 at%. This result is somewhat surprising; the magnetic structures developing in $Ni_3V_2O_8$ are sensitive to next-nearest-neighbor interactions,[13] which might be expected to be strongly affected by such a large fraction of magnetic dopants.

We followed a similar experimental procedure to probe the stability of phase transitions for Cu-doped $Ni_3V_2O_8$ by using dielectric, heat capacity, and magnetic measurements. These investigations focused on the Ni-rich compositions to probe the suppression of the multiferroic phase. Figure 4(a) plots the heat capacity of pure $Ni_3V_2O_8$ together with select $(Ni_{1-x}Cu_x)_3V_2O_8$ samples to $x = 0.13$. The curves have been offset between 0.6 and 0.8 units vertically for clarity. The two higher temperature magnetic phase transitions persist until $x \sim 0.1$, but only one transition survives and is observed for $x \sim 0.13$. Dielectric measurements, shown for the Cu-doped samples in Fig. 4(b), show a clear dielectric anomaly persists to $x = 0.05$ for $(Ni_{1-x}Cu_x)_3V_2O_8$ but vanishes at $x = 0.1$. This suggests that the ferroelectric behavior is completely suppressed on doping with 10 at% Cu. Low temperature magnetization measurements, plotted in units of μ_B per transition metal ion in Fig. 4(c), show that the magnetic moment of the samples increases with Cu fraction up to $x \sim 0.2$. Unlike pure $Ni_3V_2O_8$, samples having a small Cu fraction show a sizeable net magnetic moment in the ferroelectric phase. This result is significant because it suggests that it may be possible to obtain a net ferroelectric polarization simultaneously with a net magnetization in this system. Above $x \sim 0.1$ the rapid increase of magnetization in the ordered phase, as well as the onset of nonzero magnetization moving toward higher temperatures, suggests that the $Cu_3V_2O_8$-type magnetic structure is present and that the $Ni_3V_2O_8$ magnetic
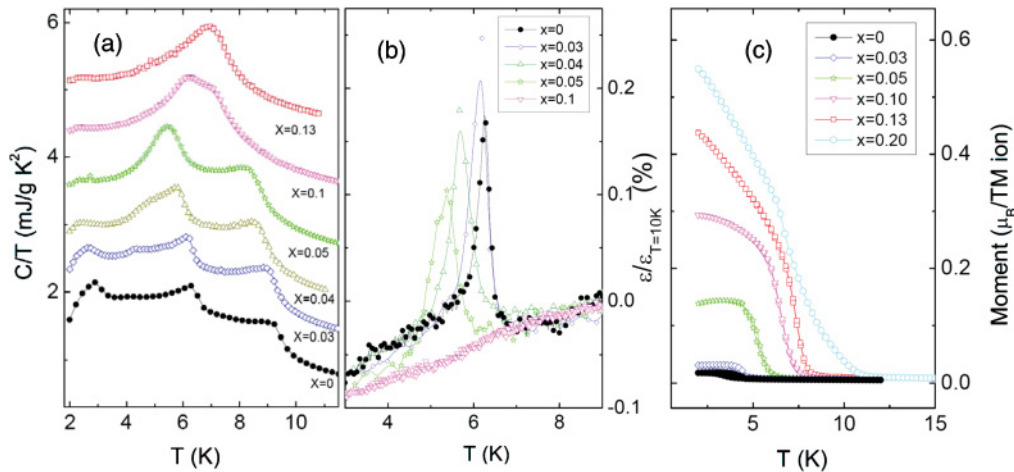
FIG. 4. (Color online) (a) Heat capacity measurements for several Cu-substituted $Ni_3V_2O_8$ samples, as indicated. The curves have been vertically offset for clarity. (b) Dielectric constant measured as a function of temperature for different compositions of Cu-substituted $Ni_3V_2O_8$. The values plotted are scaled to those measured at $T = 10$ K. (c) Magnetization measured as a function of temperature for several Cu-substituted $Ni_3V_2O_8$ samples.

structures are completely destroyed. Rather unexpectedly, these results suggest that doping with spin-1/2 Cu more strongly suppresses the magnetic transition temperatures in $Ni_3V_2O_8$ than doping with spin-3/2 Co.

In order to directly compare the effects of the different dopants on the magnetic phases of $Ni_3V_2O_8$, we plot a combined phase diagram for $(Ni_{1-x}Co_x)_3V_2O_8$ for $x = 0$ to $x = 1$ and $(Ni_{1-x}Cu_x)_3V_2O_8$ for $x = 0$ to $x = 0.5$ in Fig. 5, constructed by extracting peak positions from dielectric, magnetic, and heat capacity measurements. This phase diagram is presented as a gatefold figure with the chemical composition varying along the horizontal axis. The phase transitions extracted from dielectric measurements are shown as open triangles, while the phase transitions determined from heat capacity data are shown as solid circles, and the transitions determined from magnetic measurements for $x > 0.13$ for Cu doping as open stars. The dotted lines are included as guides-to-the-eye, and the shaded region indicates
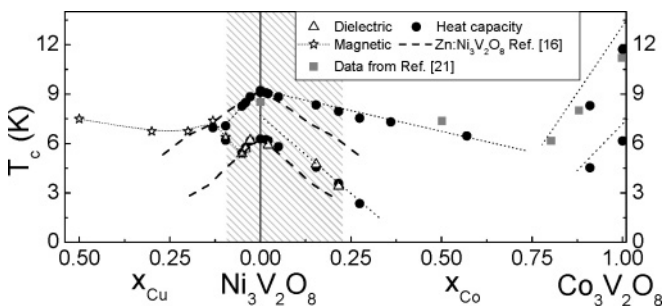
the compositional range developing multiferroic order above 2 K. All sets of measurements agree very well for the HTI-LTI phase transition. Figure 5 also includes the magnetic ordering temperature for $(Ni_{1-x}Co_x)_3V_2O_8$ for different compositions measured by Zhang *et al.*[21] (gray squares), which are in good qualitative agreement with our results. The Zn-substituted $Ni_3V_2O_8$ phase boundaries, shown as dashed lines on both sides of the fold, are presented to allow a comparison with the suppression arising from nonmagnetic dopants.

The magnetic transitions in $Ni_3V_2O_8$ doped with spin-3/2 Co show a relatively linear decrease in transition temperatures with an increasing Co percentage. The minimum in the Neel temperature, which we estimate to be just below 6 K near $x = 0.80$, is also in good agreement with previous investigations.[21] The suppression of magnetic order on doping is much more pronounced on the Co-rich side of the phase diagram than on the Ni-rich side. Surprisingly, the suppression in transition temperatures on doping with spin-3/2 Co is smaller than that obtained on doping with spin-0 Zn.

The initial rate of suppression in the transition temperatures is larger for Cu doping than for Co doping, with the reduction in transition temperatures on Cu doping approaching that observed for Zn doping. Above approximately 5 at% Cu, the heat capacity peak associated with the HTI to LTI transition in pure $Ni_3V_2O_8$ shifts to higher temperatures while the onset of magnetic ordering continues to be suppressed to lower temperatures. At 13 at% Cu doping, we observe only one clear magnetic ordering transition reaching a minimum transition temperature near $x \sim 0.2$. This suggests that the magnetic structure for even modest Cu fractions may be closer to that found in $Cu_3V_2O_8$. This is unlike the situation for Co doping, where we did not find any evidence for $Co_3V_2O_8$ magnetic phases emerging until $x \sim 0.8$.

The multiferroic transition temperature in $Ni_3V_2O_8$ is robust against doping with nonmagnetic ions.[16] On doping with magnetic ions this transition temperature can be relatively stable, for example, with Co substitution, or show considerable suppression, as observed with Cu doping. In

FIG. 5. (Color online) Composite phase diagram for Cu- and Co-substituted $Ni_3V_2O_8$. The left panel shows the transition temperatures determined from the measurements listed for Cu-substituted $Ni_3V_2O_8$. The right panel shows the transition temperature for Co-substituted $Ni_3V_2O_8$. The dashed lines indicated the transition temperatures found for $Ni_3V_2O_8$ substituted with nonmagnetic Zn, and the hashed region indicates the composition range that appears to exhibit coexisting magnetic and ferroelectric order.

order to controllably tune the properties of $Ni_3V_2O_8$ and similar multiferroics through doping, it will be crucial to understand the mechanisms affecting the suppression of the ferroelectric transition temperature and, in particular, explain the qualitatively different behaviors observed on doping Co and Cu. One possibility is that the development of a net ferromagnetic moment in $Ni_3V_2O_8$ with Cu doping, as shown in Fig. 4(c), acts to quench the ferroelectricity. Introducing a weak ferromagnetic component through doping has been shown to modify the magnetic symmetry and strongly affect the magnetoelectric coupling in other systems.[31] The onset of weak ferromagnetism in the CAF phase of undoped $Ni_3V_2O_8$ destroys the ferroelectric order, although this is typically associated with the vanishing of the inversion symmetry breaking LTI magnetic structure. However, attributing the rapid suppression of the multiferroic transition temperature in Cu-substituted $Ni_3V_2O_8$ to the emergence of a ferromagnetic moment does not explain the similarly rapid decrease of T_C in Fe-substituted $MnWO_4$, since no net magnetization develops in this system.[24]

Another possibility, motivated by the compositional phase diagram shown in Fig. 5, is that the $Cu_3V_2O_8$ magnetic structure is more stable against doping than the $Ni_3V_2O_8$ magnetic structure, which is in turn more stable than the $Co_3V_2O_8$ structure. While this explanation is unsatisfying, as it depends on estimating the energetics of these different spin structures, we note that the magnetic ordering temperature of $T_N = 29$ K[32] for $Cu_3V_2O_8$ is significantly larger than the ordering temperature for $Ni_3V_2O_8$ (9 K, Ref. 12) or $Co_3V_2O_8$ (11 K, Ref. 29), which could be consistent with a more stable magnetic structure. This suggestion could be checked by mapping out the phase diagram for Co-substituted $Cu_3V_2O_8$, which we would expect to agree with that measured for pure $Cu_3V_2O_8$ until relatively large Co fractions are introduced. Furthermore, the quantitatively different suppression in the ferroelectric suppression in $MnWO_4$ on Fe[24] and Co[25] doping can also be attributed to the emergence of new spin structures, particularly for Co doping, which suggests that the stability of the multiferroic phase may depend sensitively on the detailed nature of the dopants.

Finally, these measurements offer the tantalizing possibility that Cu-substituted $Ni_3V_2O_8$ may be simultaneously ferroelectric and exhibit a small net magnetization, at least over some small range of temperatures and compositions. This opens the possibility of controlling the ferroelectricity through coupling to a ferromagnetic, rather than antiferromagnetic, spin structure. This would allow the response to be more readily tuned using an applied magnetic field and for the magnetic structure to be probed using magnetometry rather than neutron scattering. Moreover, if the strong suppression of the multiferroic transition temperature on Cu doping can be understood, this may also suggest a route for introducing weak ferromagnetic properties in other multiferroic systems through doping with judiciously selected magnetic ions.

In summary we have investigated the phase diagram of polycrystalline Cu and Co substituted $Ni_3V_2O_8$ samples using thermodynamic, dielectric, and magnetic measurements. Consistent with previous studies, we find a minimum of the Neel temperature in $(Co,Ni)_3V_2O_8$ for Co fractions near $x = 0.75$. We also find that the suppression of the multiferroic transition temperature on doping with magnetic Co ions approximately tracks the suppression measured previously on doping with nonmagnetic Zn. Cu doping produces a much larger change in the magnetic transition temperatures, with the multiferroic phase vanishing for Cu fractions near $x = 0.1$. Although the reasons for this qualitatively different behavior on Co and Cu doping remain obscure, the observation that Cu substitution can produce a state that exhibits a ferroelectric polarization with a net magnetization highlights the possibility of introducing new magnetic functionalities into multiferroics through magnetic doping.

ACKNOWLEDGMENTS

---

*av4599@wayne.edu

[1]S.-W. Cheong and M. Mostovoy, Nat. Mater. **6**, 13 (2007).

[2]R. Ramesh and N. A Spaldin, Nat. Mater. **6**, 21 (2007).

[3]T. Kimura, G. Lawes, T. Goto, Y. Tokura, and A. P. Ramirez, Phys. Rev. B **71**, 224425 (2005).

[4]T. Goto, T. Kimura, G. Lawes, A. P. Ramirez, and Y. Tokura, Phys. Rev. Lett. **92**, 257201 (2004).

[5]S. Harikrishnan, S. Roßler, C. M. N. Kumar, H. L. Bhat, U. K. Roßler, S. Wirth, F. Steglich, and S. Elizabeth, J. Phys.: Condens. Matter **21**, 096002 (2009).

[6]D. O'Flynn, C. V. Tomy, M. R. Lees, and G. Balakrishnan, Journal of Physics: Conference Series **200**, 012149 (2010).

[7]Y. Noda, H. Kimura, M. Fukunaga, S. Kobayashi, I. Kagomiya, and K. Kohn, J. Phys.: Condens. Matter **20**, 434206 (2008).

[8]T. C. Hana and J. G. Lin, J. Magn. Magn. Mater. **310**, 355 (2007).

[9]T. Zhao, A. Scholl, F. Zavaliche, K. Lee, M. Barry, A. Doran, M. P. Cruz, Y. H. Chu, C. Ederer, N. A. Spaldin, R. R. Das, D. M. Kim, S. H. Baek, C. B. Eom, and R. Ramesh, Nat. Mater. **5**, 823 (2006).

[10]V. A. Khomchenko, D. A. Kiselev, M. Kopcewicz, M. Maglione, V. V. Shvartsman, P. Borisov, W. Kleemann, A. M. L. Lopes, Y. G. Pogorelov, J. P. Araujo, R. M. Rubinger, N. A. Sobolev, J. M. Vieira, and A. L. Kholkin, J. Magn. Magn. Mater.. **321**, 1692 (2009).

[11]J. Andres, M. Cagigas, D. S. Candela, and E. Baggio-Saitovitch, Journal of Physics: Conference Series **200**, 012134 (2010).

[12]G. Lawes, A. B. Harris, T. Kimura, N. Rogado, R. J. Cava, A. Aharony, O. Entin-Wohlman, T. Yildirim, M. Kenzelmann, C. Broholm, and A. P. Ramirez, Phys. Rev. Lett. **95**, 087205 (2005).

[13]G. Lawes, M. Kenzelmann, N. Rogado, K. H. Kim, G. A. Jorge, R. J. Cava, A. Aharony, O. Entin-Wohlman, A. B. Harris, T. Yildirim, Q. Z. Huang, S. Park, C. Broholm, and A. P. Ramirez, Phys. Rev. Lett. **93**, 247201 (2004).

[14]A. B. Harris, T. Yildirim, A. Aharony, and O. Entin-Wohlman, Phys. Rev. B **73**, 184433 (2006).

[15] L. I. Vergara, J. Cao, N. Rogado, Y. Q. Wang, R. P. Chaudhury, R. J. Cava, B. Lorenz, and J. L. Musfeldt, Phys. Rev. B **80**, 052303 (2009).

[16] P. Kharel, A. Kumarasiri, A. Dixit, N. Rogado, R. J. Cava, and G. Lawes, Philos. Mag. **89**, 1923 (2009).

[17] L. Meddar, M. Josse, P. Deniard, C. La, G. Andre, F. Damay, V. Petricek, S. Jobic, M. H. Whangbo, M. Maglione, and C. Payen, Chem. Mater. **21**, 5203 (2009).

[18] R. P. Chaudhury, F. Ye, J. A. Fernandez-Baca, B. Lorenz, Y. Q. Wang, Y. Y. Sun, H. A. Mook, and C. W. Chu, Phys. Rev. B **83**, 014401 (2011).

[19] A. A. Mukhin, V. Yu. Ivanov, A. M. Kuzmenko, A. S. Prokhorov, A. A. Pronin, S. N. Barilo, G. L. Bychkov, and S. V. Shiryaev, JETP Lett. **91**, 147 (2010).

[20] N. Qureshi, H. Fuess, H. Ehrenberg, T. C. Hansen, C. Ritter, K. Prokes, A. Podlesnyak, and D. Schwabe, Phys. Rev. B **74**, 212407 (2006).

[21] Q. Zhang, W. Knafo, K. Grube, H. V. Lohneysen, C. Meingast, and T. Wolf, Physica B **403**, 1404 (2008).

[22] Q. Zhang, W. Knafo, P. Adelmann, P. Schweiss, K. Grube, N. Qureshi, Th. Wolf, H. v. Lohneysen, and C. Meingast, e-print arXiv: 1107.2230v1, submitted (2011).

[23] R. Szymczak, M. Baran, J. Fink-Finowicki, B. Krzymanska, P. Aleshkevych, H. Szymczak, S. N. Barilo, G. L. Bychkov, and S. V. Shiryaev, J. Non-Crystalline Solids **354**, 4186 (2008).

[24] R. P. Chaudhury, B. Lorenz, Y. Q. Wang, Y. Y. Sun, and C. W. Chu, New J. Phys. **11**, 033036 (2009).

[25] R. P. Chaudhury, F. Ye, J. A. Fernandez-Baca, Y. Q. Wang, Y. Y. Sun, B. Lorenz, H. A. Mook, and C. W. Chu, Phys. Rev. B **82**, 184422 (2010).

[26] T. Lancaster, S. J. Blundell, P. J. Baker, D. Prabhakaran, W. Hayes, and F. L. Pratt, Phys. Rev. B **75**, 064427 (2007).

[27] N. Rogado, M. K. Haas, G. Lawes, D. A. Huse, A. P. Ramirez, and R. J. Cava, J. Phys. Condens. Matter **15**, 907 (2003).

[28] M. Kenzelmann, A. B. Harris, A. Aharony, O. Entin-Wohlman, T. Yildirim, Q. Huang, S. Park, G. Lawes, C. Broholm, N. Rogado, R. J. Cava, K. H. Kim, G. Jorge, and A. P. Ramirez, Phys. Rev. B **74**, 014429 (2006).

[29] N. Rogado, G. Lawes, D. A. Huse, A. P. Ramirez, and R. J. Cava, Solid State Commun. **124**, 229 (2002).

[30] N. R. Wilson, O. A. Petrenko, and G. Balakrishnan, J. Phys.: Condens. Matter **19**, 145257 (2007).

[31] D. L. Fox, D. R. Tilley, and J. F. Scott, Phys. Rev. B **21**, 2926 (1980).